

## Bond excitations in the pseudogap phase of the Hubbard model

Alexandru Macridin and M. Jarrell

*University of Cincinnati, Cincinnati, Ohio 45221, USA*

(Received 6 November 2008; published 2 December 2008)

Using the dynamical cluster approximation, we calculate the correlation functions associated with the nearest-neighbor bond operator which measure the  $z$  component of the spin exchange in the two-dimensional Hubbard model with  $U$  equal to the bandwidth. We find that in the pseudogap region, the local bond susceptibility diverges at  $T=0$ . This shows the existence of degenerate bond spin excitation and implies quantum criticality and bond order formation when long-range correlations are considered. The strong correlation between excitations on parallel neighboring bonds suggests bond singlet dimerization. The suppression of divergence for  $n < \approx 0.78$  implies that for these model parameters, this is a quantum critical point which separates the unconventional pseudogap region characterized by bond order from a conventional Fermi liquid.

DOI: 10.1103/PhysRevB.78.241101

PACS number(s): 71.10.Fd, 75.40.Mg, 74.72.-h, 74.25.Jb

### I. INTRODUCTION

The low doping pseudogap (PG) region of the cuprates has remained an issue of great discussion and controversy, with experimental data showing anomalous behaviors such as the suppression of spin excitations in the susceptibility, a PG in the single-particle spectra, and patterns in the scanning tunnel microscope (STM) spectra, among others.<sup>1,2</sup> While some investigators attributed the origin of the PG to antiferromagnetic (AF) correlations<sup>3</sup> or superconducting and/or density wave fluctuations,<sup>4</sup> others argued that the PG is due to the establishment of order.<sup>5-9</sup> In the latter scenario the optimal doping is in the proximity of the quantum critical point (QCP) associated with this order.<sup>8</sup> Previously<sup>10</sup> we investigated the staggered flux order in the PG region of single-band Hubbard model, as proposed by Chakravarty *et al.*<sup>5</sup> Despite the clear evidence of the PG signature in both one-particle density of states (DOS) and two-particle magnetic spectrum, similar to experimental data in cuprates, we found no evidence of staggered flux order.

Here we investigate a different kind of order associated with spin bond correlations. Spin bond order states were proposed to take place in the PG region.<sup>9,11-13</sup> These bond orders require the investigation of four-particle susceptibilities, which is presently very difficult to calculate with our method. However, while our method does not allow an exhaustive investigation of bond order states, we find compelling evidence that in the PG region the bond magnetic degrees of freedom should order.

Investigating the local bond excitation susceptibility with the dynamical cluster approximation (DCA),<sup>14,15</sup> we find evidence of quantum criticality in the two-dimensional (2D) Hubbard model. We consider the Coulomb interaction  $U$  to be equal to the bandwidth  $W=8t$ . The DCA is a cluster mean-field theory which maps the original lattice model onto a periodic cluster of size  $N_c=L_c^2$  embedded in a self-consistent host. Spatial correlations up to a range  $L_c$  are treated explicitly, while those at longer length scales are described at the mean-field level. However the correlations in time, essential for local criticality, are treated explicitly for all cluster sizes. We measure the fluctuations associated with the nearest-neighbor bond operator which measure the  $z$

component of spin exchange on the bond. We find degenerate bond spin excitations in the doping range  $0\% - \approx 22\%$  corresponding to the PG region, which results in a divergent local bond susceptibility at  $T=0$ . This divergence is caused by ordering in imaginary time rather than the more familiar ordering in space, and it is associated with the establishment of long-range order at a general phase transition. Nevertheless, in the limit  $N_c \rightarrow \infty$  one should expect that long-range bond correlations will quench the entropy and a transition to a state with long-range order will take place,<sup>16</sup> unless a stronger instability such as  $d$ -wave pairing occurs first. The DCA method, which does not allow spatial ordering on distances larger than the cluster size, will fail to capture this transition when small clusters are considered. However at temperatures larger than the ordering temperature the physics would be determined predominantly by the local quantum fluctuations described with DCA. The divergent behavior of bond susceptibility is suppressed for doping  $>22\%$  implying that for these model parameters,  $22\%$  doping is a QCP which separates the unconventional pseudogap region characterized by bond order from a conventional Fermi liquid. We also find a strong correlation between excitations on parallel neighboring bonds, which suggests that the pseudogap region is characterized by bond singlet dimerization.

### II. FORMALISM

To solve the cluster problem we use the Hirsch-Fye quantum Monte Carlo (QMC) method<sup>17</sup> which is based on a discrete path-integral approximation with time step  $\Delta\tau$ . Hirsch-Hubbard-Stratonovich (HHS) fields are introduced to decouple the interaction<sup>18</sup>

$$\exp(-\Delta\tau U n_\uparrow n_\downarrow + \Delta\tau U (n_\uparrow + n_\downarrow)/2) = \frac{1}{2} \text{Tr}_\sigma e^{2\alpha\sigma(n_\uparrow - n_\downarrow)}, \quad (1)$$

where an Ising HHS decoupling field  $\sigma = \pm 1$  is introduced at each spin-time location on the cluster. This transforms the problem of interacting electrons to one of noninteracting particles coupled to time-dependent fields. The fermionic fields are then integrated out, and the integrals over the HHS decoupling fields are performed with a Monte Carlo algorithm.

All measurable quantities are completely determined by the HHS fields and the host Green's function. The HHS fields contain all information about correlations (spin, pair, and charge) in space and time. Moreover, Hirsch<sup>18,19</sup> showed that spin correlations may be directly rewritten in terms of the HHS decoupling fields. One may interpret the Ising fields as representing the fermion spin variables

$$[n(i, \tau)_\uparrow - n(i, \tau)_\downarrow] \rightarrow (1 - e^{-\Delta\tau U})^{-1/2} \sigma(i, \tau). \quad (2)$$

Note that this is an exact mapping, so that all correlation functions of the HHS fields are, up to a proportionality constant, equivalent to the corresponding correlation functions of  $S^z(i, \tau) = \frac{1}{2}[n(i, \tau)_\uparrow - n(i, \tau)_\downarrow]$ .

In the DCA the one-particle and the two-particle lattice response functions are calculated with the Dyson equation using the irreducible cluster self-energy and vertices, respectively. The divergent lattice two-particle susceptibilities indicate phase boundaries. Even when a small  $2 \times 2$  cluster is considered, DCA yields regions of AF,  $d$ -wave superconductivity, and PG, similar to the generic phase diagram of cuprates (see Fig. 5 in Ref. 20). However ordering associated with more complex operators, such as valence bond singlets,<sup>9</sup> is far more difficult to detect with the DCA since it involves complex equations and up to eight-leg irreducible interaction vertices. More feasible calculations involve the corresponding cluster susceptibilities since they can be obtained directly in the QMC process. However, these cluster susceptibilities are finite-size quantities and can diverge only at zero temperature (i.e., infinite imaginary time when ordering in time occurs).

To study bond correlations, we define the bond “ $ij$ ” operator at time  $\tau$  as

$$B(i, j; \tau) = \sigma(i, \tau) \sigma(j, \tau) \propto S^z(i, \tau) S^z(j, \tau), \quad (3)$$

where “ $i$ ” and “ $j$ ” label the position in the cluster. For simplicity, we also denote with  $B_{nn}$  ( $B_{nnn}$ ) the bond operator when  $i$  and  $j$  are (next) nearest-neighbor sites.

In Sec. III we present results for the following correlation functions:

$$\chi_0(T) = \int d\tau \langle \delta B(i; i + \hat{x}, \tau) \delta B(i; i + \hat{x}, 0) \rangle, \quad (4)$$

$$\chi_\perp(T) = \int d\tau \langle \delta B(i; i + \hat{x}, \tau) \delta B(i; i + \hat{y}, 0) \rangle, \quad (5)$$

$$\chi_\parallel(T) = \int d\tau \langle \delta B(i; i + \hat{x}, \tau) \delta B(i + \hat{y}; i + \hat{x} + \hat{y}, 0) \rangle, \quad (6)$$

where

$$\delta B(i; i + \hat{x}, \tau) = B(i; i + \hat{x}, \tau) - \langle B_{nn} \rangle. \quad (7)$$

These correlation functions describe the response of the system to an external field which couples with the bond operator  $B_{nn}$ . The field acts to modify the  $z$  component of the nearest-neighbor exchange interaction. Depending on its sign it decreases or increases the energy of an AF bond and has an opposite effect on a ferromagnetic (FM) bond.  $\chi_0$  describes

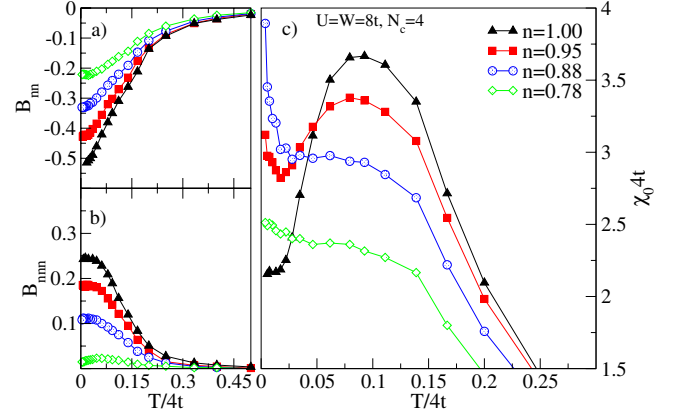


FIG. 1. (Color online) (a) and (b) Nearest (next-nearest) neighbor bond expectation value  $B_{nn}$  ( $B_{nnn}$ ) versus  $T$  for different fillings  $n$ . Short-range AF order is present in the system. (c) Local bond susceptibility  $\chi_0$  versus  $T$ .  $\chi_0$  shows a divergent behavior when  $T \rightarrow 0$  in the pseudogap region indicating critical behavior.

the local bond response while  $\chi_\perp$  and  $\chi_\parallel$  describe the correlation between nearest-neighbor bonds.

The bond correlation functions are sensitive to both single-spin fluctuations and two-spin entangled excitations. To investigate the nature of the bond excitations we introduce the fourth-order spin cumulant functions

$$F_{\langle ij \rangle \langle kl \rangle}(\tau) = \langle \sigma(i, \tau) \sigma(j, \tau) \sigma(k, 0) \sigma(l, 0) \rangle - \langle \sigma(i, \tau) \sigma(j, \tau) \rangle \times \langle \sigma(k, 0) \sigma(l, 0) \rangle - \langle \sigma(i, \tau) \sigma(k, 0) \rangle \langle \sigma(j, \tau) \sigma(l, 0) \rangle - \langle \sigma(i, \tau) \sigma(l, 0) \rangle \langle \sigma(j, \tau) \sigma(k, 0) \rangle, \quad (8)$$

$$F_0(T) = \int d\tau F_{\langle i, i+x \rangle \langle i, i+x \rangle}(\tau). \quad (9)$$

Note that  $F_{\langle ij \rangle \langle kl \rangle}$  is the correlation function between the bonds  $\langle ij \rangle$  and  $\langle kl \rangle$  with the single-spin fluctuation terms [the last two terms in Eq. (8)] subtracted off.

### III. RESULTS

We first present calculations on a  $2 \times 2$  cluster, the smallest cluster capable of reproducing the generic features of the cuprate phase diagram. In the doping region relevant for high- $T_c$  cuprates, the Hubbard model shows evidence of short-range AF correlations. The expectation value of (next) nearest-neighbor bond operator  $B_{nn}$  ( $B_{nnn}$ ) is negative (positive) and increases with lowering temperature, as one expects for a system with short-range AF order. The short-range AF order is stronger at smaller doping.  $B_{nn}$  and  $B_{nnn}$  versus temperature at different fillings are shown for a  $N_c=4$  cluster in Figs. 1(a) and 1(b), respectively.

In the electron-density range  $1 > n > \sim 0.78$ , the temperature dependence of the local bond susceptibility shows the existence of degenerate or almost degenerate states with different magnitude of their bond value  $B_{nn}$ . It is interesting that this doping range corresponds to the pseudogap region of an  $N_c=4$  cluster (see Fig. 5 in Ref. 20). As shown in Fig. 1(c) the extrapolation of our data indicates that  $\chi_0$  is diverging

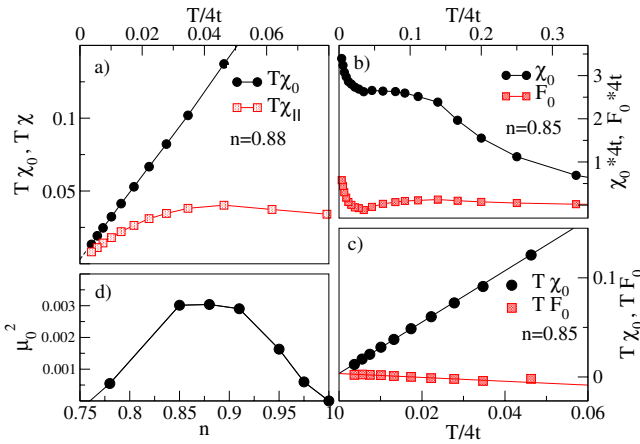


FIG. 2. (Color online) (a)  $T\chi_0(T)$  shows a linear behavior and extrapolates to a finite value  $\mu_0^2$  at  $T=0$ . (b) and (c) Both the local bond susceptibility  $\chi_0(T)$  and the local cumulant  $F_0(T)$  diverge as  $\frac{\mu_0^2}{T}$  when  $T \rightarrow 0$ , showing that the low-temperature regime is characterized by entangled two-spin excitations. (d)  $\mu_0^2$  versus filling  $n$ .

when  $T \rightarrow 0$ . Since the lowest temperature we can reach is  $\approx 0.01t$  the apparent divergent  $\chi_0$  implies, if not degenerate states, at least bond excitations with an energy much smaller than this scale.

In the pseudogap region (i.e.,  $1 > n > \sim 0.78$ )  $\chi_0$  diverges as  $\sim \frac{1}{T}$ . This can be seen in Fig. 2(a) where we show (black line)  $T\chi_0$  versus  $T$  at filling  $n=0.88$ .  $T\chi_0$  displays a linear behavior, and at  $T=0$ , it extrapolates to a finite value, albeit small,  $\mu_0^2$ . The  $\sim \frac{1}{T}$  dependence of susceptibility is consistent with scenarios which assume two degenerate configurations, 1 and 2, with different bond values such that  $2\mu_0 = B_{nm}(1) - B_{nm}(2)$ . It is instructive to draw an analogy with local spin susceptibility of a system with independent local moments. A free moment is a doubly degenerate problem where the spin can be aligned parallel or antiparallel to a particular direction. A perturbing magnetic field lifts the degeneracy of the two configurations by an amount proportional to the moment and the magnetic field. Similarly, in our system the perturbing Hamiltonian acting on the bond  $\langle ij \rangle$ ,  $H^{\text{ext}} = hB(i, j)$ , splits the two configurations with an amount proportional to the field  $h$  and  $B(i, j)(1) - B(i, j)(2)$ . Thus, the  $\sim \frac{1}{T}$  dependence of the local bond susceptibility suggests the existence of two degenerate states with different bond magnitude. Of course other scenarios compatible with a  $\sim \frac{1}{T}$ -like susceptibility cannot be excluded.

It is interesting that the divergence of the bond susceptibility is not due to single-spin flips since the fourth-order spin cumulant shows a similar divergence. This can be seen in Fig. 2(b) where both the local bond  $\chi_0(T)$  and the local cumulant  $F_0(T)$  are shown. They both diverge like  $\frac{\mu_0^2}{T}$  since  $T\chi_0(T)$  and  $TF_0(T)$  intersect exactly at  $T=0$  [see Fig. 2(c)], which we find to be true at all dopings in the pseudogap region. Therefore the low-temperature regime is characterized by entangled two-spin excitations rather than by simple single-spin ones.

The bond correlations are strongest around  $n \approx 0.88$  and weak at small and large dopings. This can be seen both by inspecting  $\chi_0(T)$  in Fig. 1(b) and by looking at the bond

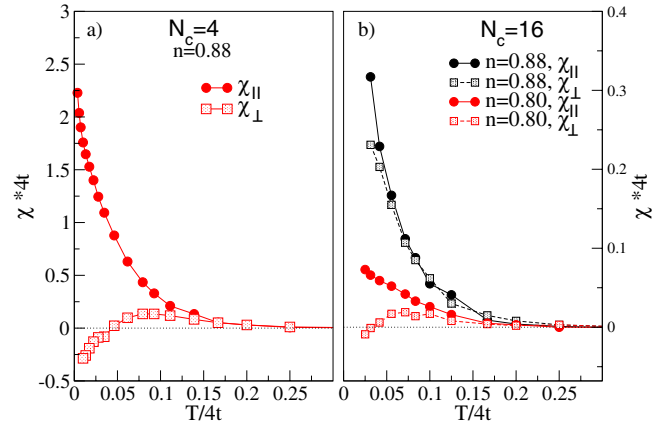


FIG. 3. (Color online) (a)  $\chi_{\parallel}$  and  $\chi_{\perp}$  versus  $T$  for  $N_c=4$  at  $n=0.88$ . (b)  $\chi_{\parallel}$  and  $\chi_{\perp}$  versus  $T$  for  $N_c=16$  at  $n=0.88$  and  $0.80$ . At low  $T$  the correlation between nearest-neighbor parallel bonds is much stronger than the correlation between nearest-neighbor perpendicular bonds.

moment  $\mu_0^2$  versus filling in Fig. 2(d). At half filling, the bond moment extrapolates to zero since the numerical data do not show evidence of divergent susceptibilities in the undoped system. At finite doping  $\mu_0^2$  increases with increasing doping displaying a maximum at  $n \approx 0.88$ .  $\mu_0^2(n)$  decreases with further doping until it vanishes at  $n \approx 0.78$ .

At low temperatures we find a strong positive correlation between nearest-neighbor parallel bonds and a small negative correlation between nearest-neighbor perpendicular bonds. This is shown in Fig. 3(a).  $\chi_{\parallel}$  is increasing strongly with lowering  $T$ ; the numerical data indicate even a possible divergence when  $T \rightarrow 0$ , although it is weaker than  $\sim \frac{1}{T}$  characteristic to local bond fluctuations [see Fig. 2(a)]. The large value of  $\chi_{\parallel}$  shows that increasing or reducing the antiferromagnetism on a bond implies a similar effect on the nearest-neighbor parallel bond, whereas the correlation between nearest-neighbor perpendicular bond fluctuations  $\chi_{\perp}$  is much smaller and negative.

Larger cluster calculations are limited to finite temperatures due to the minus-sign problem present in the Hirsch-Fye algorithm. For example, for the values of  $U/W$  used here, when  $N_c=16$  the minus-sign limits Hirsch-Fye QMC calculations to  $T \geq 0.112t$  for fillings in the pseudogap region. Unfortunately, this temperature is outside the temperature range where the bond critical behavior was noticed for  $N_c=4$ . Moreover one should expect the divergent behavior of the bond correlations to reduce with increasing the cluster size. This is due to the establishment of bond order when spatial correlations at larger length scale are incorporated, which is a similar behavior noticed previously in the local spin susceptibility.<sup>21</sup>

For the  $N_c=16$  cluster the correlation between nearest-neighbor parallel bonds is larger than the correlation between nearest-neighbor perpendicular bonds, consistent with the  $N_c=4$  results. This can be seen in Fig. 3(b), where  $\chi_{\parallel}$  and  $\chi_{\perp}$  are shown for  $N_c=16$  at two different fillings. At smaller doping,  $n=0.88$ , in the temperature range available, the behavior of the bond correlations is dominated by the strong single-spin AF fluctuations, as our analysis of both fourth-

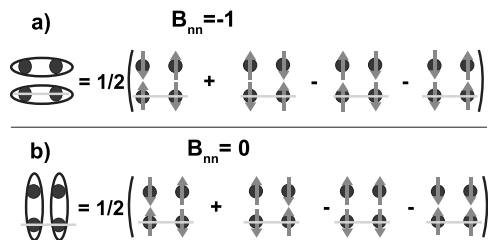


FIG. 4. (a) Configuration with bond singlets along  $x$  direction. The marked bond is a superposition of states with AF aligned spins. (b) Configuration with bond singlets along  $y$  direction. The marked bond is a superposition of two states with AF aligned spins and of two states with FM aligned spins. The bond operator, Eq. (3), measured on the bond along  $x$  direction (marked bond) takes the value  $B_{nm} = -1$  ( $B_{nm} = 0$ ) for configuration a (b). If (a) and (b) are degenerate, the local bond susceptibility and local cumulant will diverge as  $\frac{\mu_0^2}{T}$  when  $T \rightarrow 0$ .

order spin cumulant and bond correlation shows. Here  $\chi_{\perp}$  increases with decreasing  $T$  but it is slower than  $\chi_{\parallel}$ . At larger doping,  $n=0.80$ , presumably close to the QCP where the AF correlations are weak,  $\chi_{\perp}$  decreases with decreasing  $T$  and eventually becomes negative, similar to  $N_c=4$  cluster behavior.

#### IV. DISCUSSION

Without dismissing other possibilities, we note that a scenario where the system forms adjacent parallel bond singlets fits very well with our results. For instance the divergence of local bond susceptibility  $\chi_0$  requires two degenerate states with different  $B_{nm}$ . Suppose we measure  $\chi_0$  on a bond along  $x$  direction. A configuration with adjacent parallel bond singlets along  $x$ , such as the one in Fig. 4(a), has a  $B_{nm} = -1$ , while a configuration with adjacent parallel bond singlets along  $y$ , such as one in Fig. 4(b), has a  $B_{nm} = 0$ . If these two configurations are degenerate they will yield both a divergent  $\chi_0$  and a divergent  $F_0$ . Moreover the correlation between parallel bond excitations will also be divergent and positive,

while the correlation between nearest-neighbor perpendicular bonds will be negative, resembling our findings for both  $N_c = 4$  and 16 clusters.

It would be interesting to investigate the dependence of the QCP as a function of the cluster size. However, the temperature range restriction for the  $N_c=16$  calculations makes this unfeasible. A definite answer to whether there is a causal relation between the PG and the bond fluctuations or whether they just happen to coexist is also difficult to be given at this time.

#### V. CONCLUSIONS

The behavior of bond susceptibility in the PG region of the 2D Hubbard model calculated with DCA shows evidence of quantum criticality and implies establishment of bond order. Thus, in the  $2 \times 2$  cluster we find divergent local bond susceptibility at  $T=0$ , which implies ordering in the imaginary time due to the existence of degenerate bond spin excitations. We find a strong correlation between excitations on parallel neighboring bonds, which suggests that the pseudogap region is characterized by bond singlet dimerization. We argue that the existence of unquenched local zero-energy fluctuations for small  $N_c$  implies long-range order in the limit  $N_c \rightarrow \infty$  or the intervention of competing phase transition. The suppression of divergence for  $n < \approx 0.78$  implies that  $n \approx 0.78$  is a QCP which separates the unconventional pseudogap region characterized by dimers from a conventional Fermi liquid.

#### ACKNOWLEDGMENTS

This research was supported by NSF (Grants No. DMR-0312680 and No. DMR-0706379) and CMSN, DOE (Grant No. DE-FG02-04ER46129). Supercomputer support was provided by the Texas Advanced Computing Center. We would like to thank J. C. Davis, P. Hirschfeld, M. Ma, M. Norman, G. Sawatzky, and N. S. Vidhyadhiraja for stimulating conversations, and all of the organizers of the Sanibel Symposium.

<sup>1</sup>T. Timusk and B. Statt, Rep. Prog. Phys. **62**, 61 (1999).

<sup>2</sup>Y. Kohsaka *et al.*, Science **315**, 1380 (2007); Y. Kohsaka *et al.* Nature (London) **454**, 1072 (2008).

<sup>3</sup>A. P. Kampf and J. R. Schrieffer, Phys. Rev. B **42**, 7967 (1990).

<sup>4</sup>X.-G. Wen and P. A. Lee, Phys. Rev. Lett. **76**, 503 (1996).

<sup>5</sup>S. Chakravarty, R. B. Laughlin, D. K. Morr, and C. Nayak, Phys. Rev. B **63**, 094503 (2001).

<sup>6</sup>C. M. Varma, Phys. Rev. Lett. **83**, 3538 (1999).

<sup>7</sup>S. Kivelson *et al.*, Nature (London) **393**, 550 (1998).

<sup>8</sup>M. Vojta, Y. Zhang, and S. Sachdev, Phys. Rev. B **62**, 6721 (2000).

<sup>9</sup>S. Sachdev, Rev. Mod. Phys. **75**, 913 (2003).

<sup>10</sup>A. Macridin, M. Jarrell, and T. Maier, Phys. Rev. B **70**, 113105 (2004).

<sup>11</sup>N. Read and S. Sachdev, Phys. Rev. Lett. **62**, 1694 (1989).

<sup>12</sup>T. Senthil and M. P. A. Fisher, Phys. Rev. B **62**, 7850 (2000).

<sup>13</sup>S. Sachdev *et al.*, Ann. Phys. (N.Y.) **298**, 58 (2002).

<sup>14</sup>M. H. Hettler, A. N. Tahvildar-Zadeh, M. Jarrell, T. Pruschke, and H. R. Krishnamurthy, Phys. Rev. B **58**, R7475 (1998); M. H. Hettler, M. Mukherjee, M. Jarrell, and H. R. Krishnamurthy, *ibid.* **61**, 12739 (2000).

<sup>15</sup>T. Maier, M. Jarrell, T. Pruschke, and M. H. Hettler, Rev. Mod. Phys. **77**, 1027 (2005).

<sup>16</sup>Such as the transition of a Mott state with unscreened local moments into an antiferromagnetic state.

<sup>17</sup>J. E. Hirsch and R. M. Fye, Phys. Rev. Lett. **56**, 2521 (1986).

<sup>18</sup>J. E. Hirsch, Phys. Rev. B **28**, 4059 (1983).

<sup>19</sup>J. E. Hirsch, Phys. Rev. B **34**, 3216 (1986).

<sup>20</sup>M. Jarrell *et al.*, Europhys. Lett. **56**, 563 (2001).

<sup>21</sup>The  $T=0$  divergence of local spin susceptibility, present for the impurity calculations (i.e.,  $N_c=1$ ), disappears when going to finite cluster which allows the establishment of short-range AF order.